OVERDISCHARGE AND EXTERNAL SHORT BEHAVIOR OF LITHIUM-ION BATTERIES

An Undergraduate Research Scholars Thesis

by

CONNER FEAR

Submitted to the Undergraduate Research Scholars program at
Texas A&M University
in partial fulfillment of the requirements for the designation as an

UNDERGRADUATE RESEARCH SCHOLAR

Approved by Research Advisor: Dr. Partha P. Mukherjee

May 2017

Major: Mechanical Engineering

TABLE OF CONTENTS

ABSTRACT

Overdischarge and External Short Behavior of Lithium-Ion Batteries

Conner Fear
Department of Mechanical Engineering
Texas A&M University

Research Advisor: Dr. Partha P. Mukherjee
Department of Mechanical Engineering
Texas A&M University

Lithium-ion batteries (LIBs) have become increasingly popular for commercial use in recent years, however, the frequency of accidents involving LIBs raises concerns over their safety. A commonly experienced condition for batteries is an external short, which causes the cell to discharge at a high rate and, hence, at large currents, resulting in rapid heat generation in the wire as well as within the cell. Another condition, known as overdischarge, is also becoming a common safety issue as greater numbers of cells are being connected in series, as is the case in systems requiring high voltages, such as Electric Vehicles (EVs). This work seeks to explain the mechanisms that cause internal damage to cells during external shorting and overdischarge and to determine the most dangerous conditions that can exist during these types of abuse. An external short test using a commercial 18650 cell (Panasonic) was conducted by subjecting the cell to a constant resistance discharge with resistors of decreasing value (from 100-0.01 Ω). To perform the overdischarge test, a constant current discharge phase with no lower cutoff voltage was used to overdischarge the same type of cells to -100% SOC. The phenomenon of copper dissolution from the anodic current collector was observed in each overdischarged cell. Voltage, current, and temperature behavior was monitored throughout the cycling of all cells in order to determine the

cell response to the abnormal cycling. The internal damage of the cells was studied by conducting a Destructive Physical Analysis (DPA) and by analyzing cell components via Scanning Electron Microscopy (SEM). The external shorting results showed that a single 18650 cell experiencing external short can produce potentially dangerous amounts of heat when the resistance of the short is between 0.47 Ω and 1 Ω. Cracking was observed on both the anode and cathode surface of the externally shorted cell, indicating a loss of capacity. The overdischarge test results confirmed that copper dissolution occurs when the cell voltage reaches -1.1 V in the Panasonic cells. The deposition of copper on the cathode surface can lead to the trapping of lithium ions within the cathode. Loss of copper material from the anodic current collector can cause loss of adhesion of the anode material to the collector and loss of mechanical stability of the anode roll. This work will provide a better understanding of LIB behavior under abusive conditions.

DEDICATION

I would like to dedicate this work to my parents, Rich and Maureen Fear, for their unending support and encouragement throughout my academic career.

ACKNOWLEDGEMENTS

Financial support for this work was provided by Underwriters Laboratories, Texas Instruments, and the TAMU Faculty Research Initiation Grant. I would like to thank my advisor, Dr. Mukherjee, for providing me the opportunity and resources to complete this work. I would also like to thank Daniel Juarez-Robles, whose advice and assistance were instrumental to the success of this project.

NOMENCLATURE

CC	Constant Current
CV	Constant Voltage
DPA	Destructive Physical Analysis
EV	Electric Vehicle
LIB	Lithium-Ion Battery
OCV	Open Circuit Voltage
PE	Polyethylene
PP	Polypropylene
SEI	Solid-Electrolyte Interface
SEM	Scanning Electron Microscopy
SOC	State of Charge
XRD	X-Ray Diffraction

CHAPTER I

INTRODUCTION

Overview

In response to consumer demand for electric vehicles and portable electronics with greater energy storage capabilities, the market for lithium-ion batteries has experienced rapid growth in recent years. The high power, high energy density, and efficient reversibility of LIBs make them attractive choices for a variety of energy storage applications [1]. Unfortunately, the strong performance of the lithium-ion chemistry has been accompanied by the frequent occurrence of accidents, revealing the need for a more thorough understanding of the behavior of these powerful cells under abnormal conditions.

A common abuse condition experienced by LIBs is an electrical short, which occurs when the positive and negative terminals of a battery come into contact with minimal electrical resistance. This causes the cell to discharge at a high rate, thus producing large amounts of current and rapidly generating heat within the cell as well as in the external circuit. If the cell temperature is not properly controlled, very high internal temperatures (~180°C) can spur undesired exothermic reactions in the cell, known as thermal runaway, which can even lead to fire or explosion [2]. In September 2016, Samsung was forced to recall nearly 1 million Galaxy Note 7 phones after numerous reports of the devices exploding during extended charging [3]. It was later revealed that the issue stemmed from a design flaw in which the battery's external casing was too small for the internal components, causing them to short circuit. While the dangers of internal shorting in LIBs have been well-documented, few studies have focused on the response of LIBs to external shorting, which can easily occur due to faulty packaging or careless handling of cells. This study seeks to

explain the response of LIBs to an external short and to determine under what conditions this shorting could lead to damage or failure in cells.

Another condition, known as overdischarge, is becoming an increasing concern for designers of high-voltage battery packs, as required by systems such as electric vehicles. To meet these voltage requirements, greater numbers of cells are being connected in series [8]. When placed in a series arrangement, the voltage of individual batteries cannot be controlled directly; only the voltage of the full module can be adjusted. Slight differences in the manufacturing of cells can cause some cells to have less capacity than others in the series. Nevertheless, when the module is discharging, the cells with lower capacity are demanded to deliver the same amount of current as other cells. Commercial LIBs typically specify a voltage range (~2.5-4.2 V) for safe operation in order to prevent undesirable side reactions from occurring in the cell. When lower capacity cells in an unbalanced module discharge beyond their recommended lower voltage limit, overdischarge occurs and permanent capacity fade or failure can be caused. Additionally, extreme overdischarge conditions can result in the dissolution of the copper anodic current collector, which can deposit on internal cell components and induce an internal short. This condition can be very dangerous because the flow of electrical current within the cell can create localized heat zones in the highly flammable electrolyte around the conductive pathways. Cases of internal short often result in fire or explosion, which could be catastrophic in a large battery pack. This study will investigate the causes of copper dissolution during overdischarge and determine under what conditions overdischarge could become dangerous.

Objective

The objective of this work will be to study the phenomenon of copper dissolution during extreme overdischarge of Li-ion cells. Initially, a constant resistance discharge will be used to study the behavior of a commercial 18650 cell during external shorting in order to determine whether copper dissolution can occur without overdischarge beyond 0 V. Then, a study will be conducted in which cells will be subjected to overdischarge by using a constant current protocol with no lower voltage limit. This will emulate the performance of the cell when it is placed in an unbalanced load module and driven to negative polarity by the surrounding cells. Electrochemical and sensitive analysis will be conducted on the cell response. Also, post-mortem analysis and scanning electron microscopy (SEM) will be employed to determine the physical consequences of abuse due to external shorting and overdischarge.

External Short Test

When the battery terminals are connected to an external circuit, the voltage tends to drop to a value called the closed-circuit voltage due to several types of polarization. The difference between the open and closed circuit voltages for a cell is known as the overpotential, η, and is defined as $\eta = E_{OCV} - E_T$, [4], where E_{OCV} is the Open Circuit Voltage (OCV) and E_T is the terminal cell voltage with current flowing. Activation polarization is the voltage drop related to the kinetics of the charge-transfer reactions taking place at the electrode/electrolyte interfaces [4]. Ohmic polarization is the voltage drop due to the internal resistance of a cell, as dictated by Ohm's law ($V=iR$). This includes both resistances to electron and ion transfer in the cell, such as the resistance of the electrolyte to ion transfer and poor contact of conductive pathways between the reaction sites and the current collector in the electrode. Concentration polarization is caused by the

unavailability of the active species at the electrode/electrolyte interface to continue with the reaction. As the reaction proceeds, active species particles must diffuse to the electrode surface to replace the previously reacted materials. The buildup of a gradient between the electrode surface and bulk concentrations causes a voltage drop. The three polarization mechanisms discussed here are illustrated on a typical battery discharge curve in Figure 1. In constant resistance discharge the current decreases during the discharge proportionally to the decrease in the battery voltage [5]. Therefore, drops in voltage will result in proportional current drops throughout our external short tests.

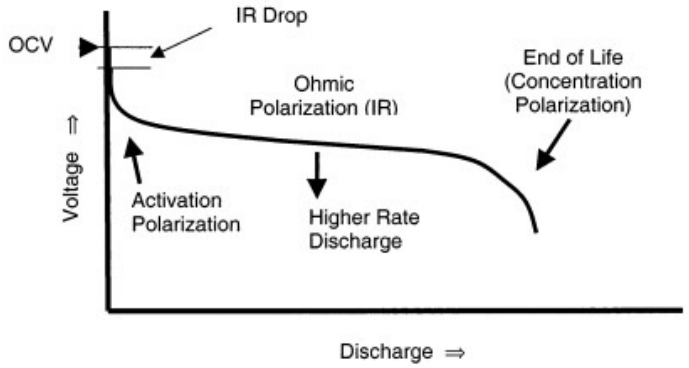

Figure 1. *Battery discharge curve, showing the influence of various types of polarization [4].*

An external short circuit abuse test on prismatic $LiCoO_2/LiC_6$ batteries was performed by Leising *et al*. using a resistance of 6 mΩ [6]. In this test, cells were fully charged to +4.1 V and externally short-circuited. The temperature of each cell was monitored by a thermocouple applied to the battery surface. Within 0.2 s of starting the test, the current peaked and the voltage dropped severely to less than 0.25 V. For the next 1.5 minutes, the current held at about 14-15 A and the temperature began to rise. At this point, the current fell to less than 2 A, but the temperature continued to steadily rise. After 3.5 min, the temperature peaked and the current began to decay to

0.0 A. The maximum surface temperatures measured by the thermocouple was 109 °C. The temperature and current profiles for this test are shown in Figure 2.

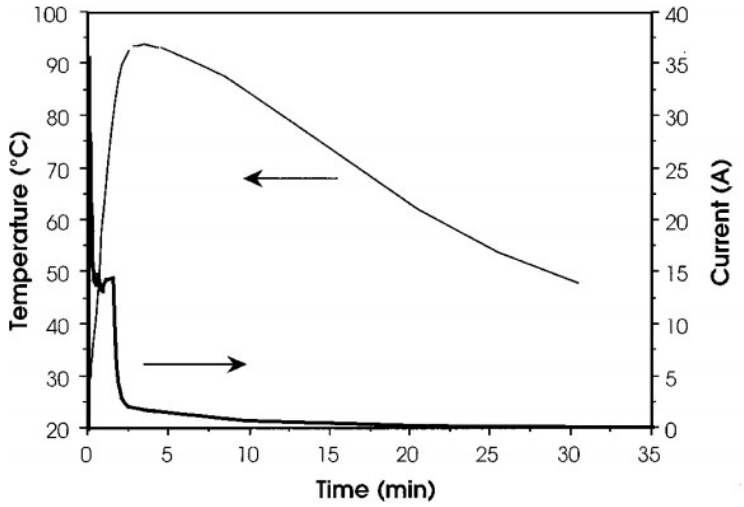

Figure 2. *Temperature and current for prismatic Li-ion cell in external short circuit test [6].*

Wu *et al.* achieved similar results in an external short-circuit on prismatic cells with a capacity of 750 mAh [7]. This test was performed on both fresh cells (10 cycles) and cells that had already suffered some abuse (200 cycles). It also considered the influence of separator material, testing cells with polyethylene (PE), polypropylene (PP), and PP/PE/PP separators. The current and temperature behavior during the test are shown in Figure 3. When the cells were shorted with an external resistance of 30 mΩ, the current peaked instantaneously at 25 A, stayed around 11 A for 70 s, and finally drops to less than 1 A. The temperature steadily rose for 70 s to a maximum of 110 °C. It is reported that results were identical for all three separators and that cycle number had a negligible effect on the behavior.

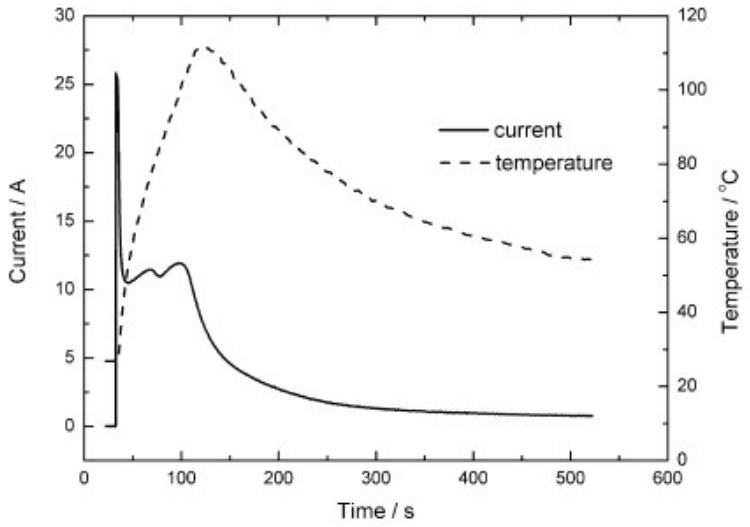

Figure 3. *Current and temperature behavior of battery in external short-circuit test after more than 200 cycles [7].*

Previous studies of external shorting have not considered the impact of external circuit resistance during shorting. The impact of utilizing an 18650 cell rather than a prismatic cell will also be a key component in this study, as different cell geometries may have varying ability to dissipate heat. Additionally, the cylindrical cells used in this study have higher capacities than the prismatic cells of previous studies, which could cause more heat generation during a short. By discharging 18650 cells under constant resistance conditions using a wide range of loads, this study will determine the resistance that creates the most dangerous conditions in the cell. It will also introduce post-mortem analysis of cell components after disassembly to investigate the damage caused by external shorting.

Overdischarge and Copper Dissolution Test

Slight differences in initial SOC between the cells in series are amplified by cycling because cells with a higher initial SOC will be repeatedly subjected to overcharge while the cells with a lower initial SOC will be repeatedly subjected to overdischarge.

The voltage change at the end of discharge in a full cell is primarily driven by the rise in voltage of the anode [8]. When the anode voltage reaches 3.5 V (vs Li/Li^+) or higher, the copper current collector of the anode can begin to oxidize to Cu^{2+} and dissolve into the electrolyte [9]. The results of a cyclic voltammetry test on copper foil in an organic electrolyte are shown in Figure 4, which shows that the rate of copper dissolution increases rapidly around 3.5 V [10]. The dissolved copper from the anodic current collector will be redeposited on the anode surface, which can form an electric shunt and increase the internal resistance of the cell [9]. At the same time, over-deintercalation of lithium at the anode causes decomposition of the solid-electrolyte interface (SEI), which generates gases, including carbon dioxide. The formation of new SEI films while recharging the cell then consumes some lithium ions, reducing the cell capacity.

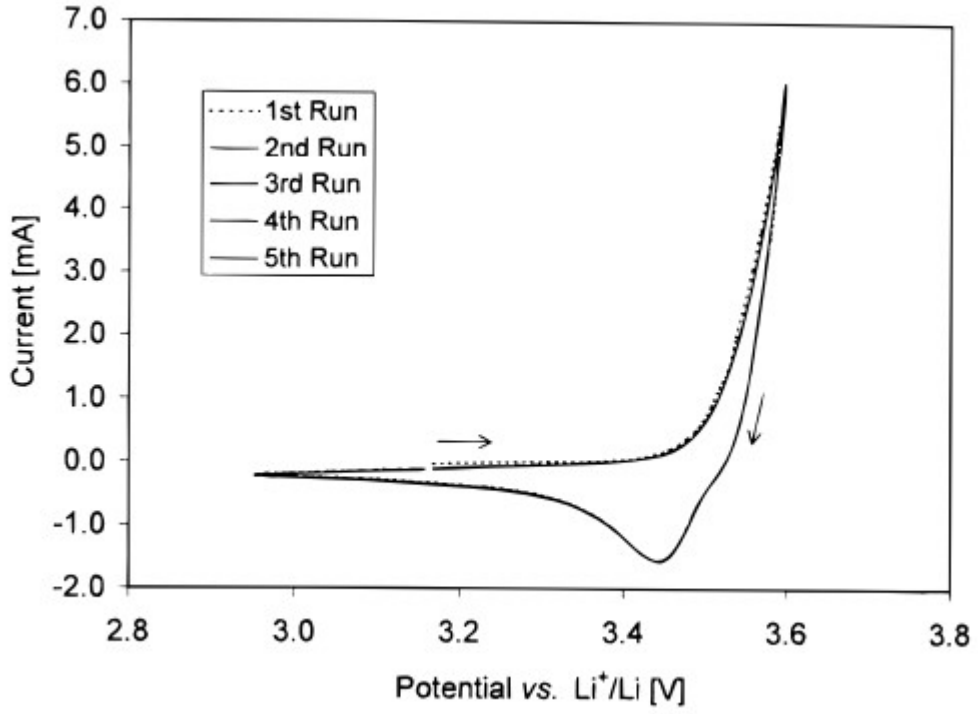

Figure 4. *Five consecutive CV cycles of a Cu foil electrode in 1M $LiPF_6$/PC:EC:DMC (1:1:3) electrolyte [10].*

In extreme overdischarge conditions, copper deposition on the cathode surface can begin to form electrically conductive pathways within the cell and can result in the formation of an internal short circuit, as illustrated in Figure 5 [9]. Guo *et al.* report that this internal short circuit can be safely and reliably induced through deep overdischarge without mechanical destruction or the introduction of foreign substances. Additionally, the side reactions that occur during extreme overdischarge result in the solid-state amorphization of transition metal compounds that make up much of the cathode material, leading to capacity degradation [9]. Other common issues that arise due to this condition are loss of adhesion between the anode material and the current collector and loss of contact between the copper sheet and the Ni lead-out tap, which may result in electronic isolation of the entire anode [8]. When Guo *et al.* attempted to recharge overdischarged cells, those

with mild internal shorting showed high rates of self-discharge, while those with severe shorting could not be fully recharged [9]. SEM and XRD results confirmed that copper deposition on both the anode and cathode was the cause of the short circuit. This study also found that neither internal short circuit nor capacity fading occurs if the overdischarge is terminated before reaching an SOC of -12%.

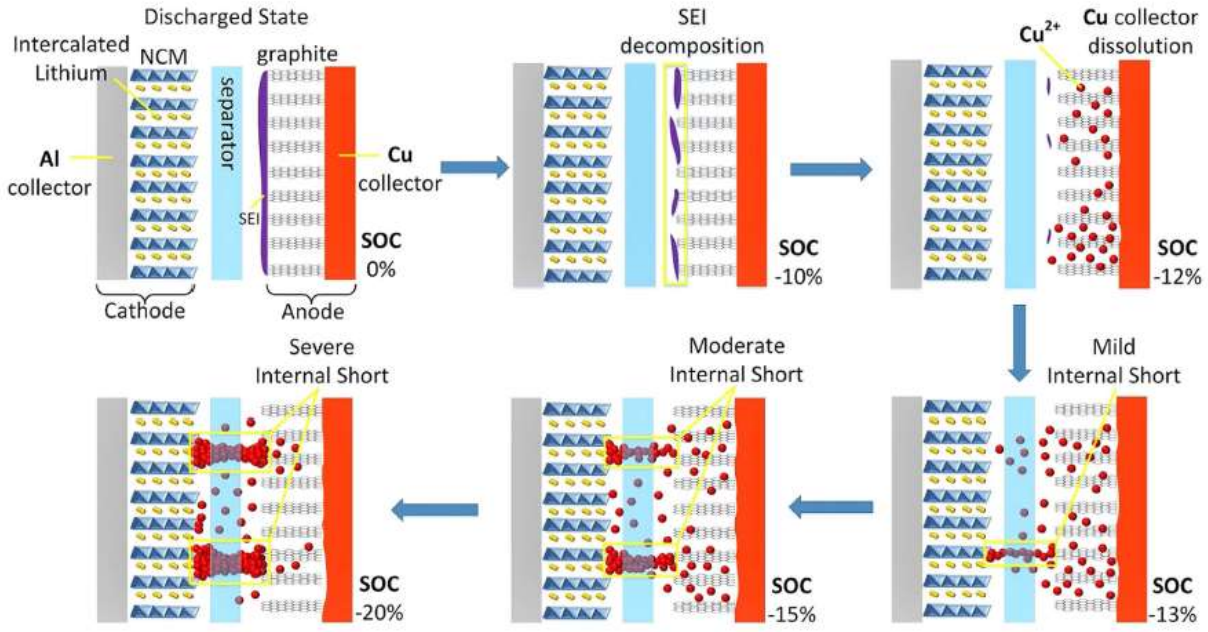

Figure 5. *Dissolution and deposition of copper during overdischarge and the formation of an internal short circuit [9].*

Maleki and Howard performed an experiment to explore the effects of overdischarge on the cycle-life and thermal stability of Li-ion cells [11]. Commercial cells, rated at 780 mAh, were overdischarged and kept at 2.0, 1.5, 1.0, 0.5, or 0.0 V for 72 h and then cycled five times. This process was repeated five times, measuring the a.c. impedance after each repetition. The cells overdischarged to voltages between 2.0 and 0.5 V experienced capacity losses of 2-16%. These

cells lost between 8% and 26% more capacity after being cycled 100 times between 3.0 and 4.2 V. Overdischarging to 0.0 V caused more severe capacity losses in some cells and caused some cells to fail entirely. Of the three failed cells, only one showed significant signs of copper dissolution. Energy-dispersive X-ray (EDX) analysis confirmed that copper was found on the cathode and separator surfaces of this cell, while all other cells contained statistically insignificant amounts of copper on these surfaces.

Kishiyama *et al.* studied the effects of 0.0 V overdischarge on Li-ion cells whose anodes used current collectors made of either titanium or copper [12]. They demonstrated that the dissolution of copper is the main cause of capacity loss in cells under this condition. Additionally, they showed that the SEI layer could break down if the anode voltage exceeds 3.5 V. Mao demonstrated that anode potential can reach as high as 3.8 V when overdischarging a Li-ion cell to 0.0 V [13]. Therefore, it is possible that both copper dissolution and breakdown of the SEI layer are causes of capacity loss during the overdischarge process [11].

To the best of the author's knowledge, few previous studies have focused on extreme overdischarge (below 0.0 V) or on the phenomenon of copper dissolution during overdischarge. In this study, the response of a single LIB to deep overdischarge was examined. A constant current discharge phase with no lower cutoff voltage was used to drive the cell voltage below 0.0 V and to reliably induce copper dissolution. The voltage and temperature behaviors of the cell were monitored throughout the test.

CHAPTER II

METHODOLOGY

Experimental Setup

External Short Test

A commercial 18650 cell was discharged repeatedly through an external circuit with various resistances ranging from 100 Ω to 0.01 Ω. High-power ceramic resistors were required for this test, as preliminary testing showed that the more common carbon resistors could melt under the load of the externally shorted cell. The voltage, current, and temperature responses of the cell were monitored and recorded throughout the discharge by an Arbin-BT2000 cycling machine. A detailed depiction of the experimental setup is shown in Figure 6.

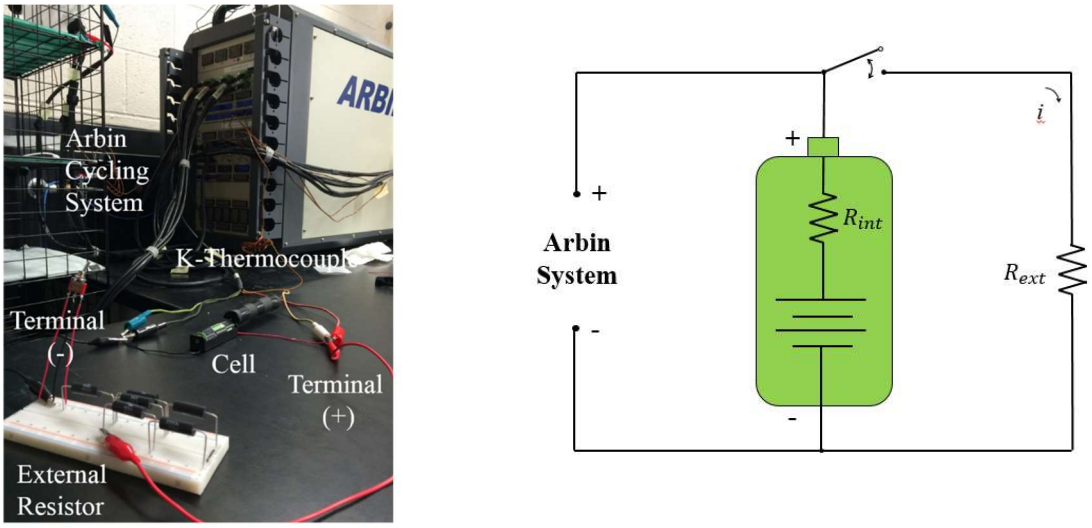

Figure 6. *(a) Experimental apparatus for external short test. Cell is connected to external resistor circuit as well as Arbin cycling machine. (b) Schematic of circuit used to complete test.*

Protocol

A – Preparation Test

1. Charge using constant current (CC) at 1C to cutoff voltage of 4.2 V
2. Charge using constant voltage (CV) at 4.2 V until current falls below 0.05 A

B – External Short Test

1. Manually short circuit cell by closing switch
2. Monitor voltage and record every 1 ms throughout discharge
3. Open switch and stop recording when voltage falls below 0.5 V

Overdischarge and Copper Dissolution Test

A commercial Panasonic NCR18650B cylindrical cell was used in this experiment. The rated capacity of the cell was 3350 mAh at 1C and 25°C. The cathode material of this cell is Nickel Cobalt Aluminum Oxide ($LiNiCoAlO_2$, NCA) and the anode material is graphite (C).

Protocol

A – Preparation Test

1. Charge using CC at C/20 rate up to 4.2 V
2. Charge using CV at 4.2 V with cutoff current of 0.05 A
3. Rest 30 min
4. Discharge using CC at C/20 rate to 50% SOC
5. Current pulse to measure internal resistance

6. Discharge CC at C/20 down to 2.5 V

5. Rest 30 min

6. Charge CC at C/20 to 4.2 V

7. Charge CV at 4.2 V with 0.05 A cutoff current

B – Overdischarge Test

1. Charge CC at C/10 to 4.2 V

2. Charge CV at 4.2 V to 0.05 A

3. Discharge CC at C/10 to 2.5 V

4. Charge CC at C/10 to 4.2 V

5. Charge CV at 4.2 V to 0.05 A

6. Discharge CC at C/10 or 1C with no lower cutoff voltage until SOC < -100%

Destructive Physical Analysis

Destructive physical analysis (DPA) was performed on all test cells in order to determine what damage had been caused to cell components. Cells were disassembled within a sealed argon glovebox for safety and to prevent reactions with the environment from affecting interior components. To safely open a commercial cell, it is important to avoid shorting the cell, as this could result in rapid heat generation. Therefore, it is recommended that cells are left in a discharged position before disassembly to minimize discharge energy in case of a short.

DPA Procedure

1. Remove plastic wrapping to expose aluminum casing.

2. Insert pipe cutter blade at seam of cell, as shown in Figure 7. Tighten until seal is broken and rotate cell until the whole cap is detached. Do not tighten pipe cutter too much, or the gasket separating the cap from the case may be punctured and the cell may short.

Figure 7. *Cell is opened by breaking the seam with a pipe cutter.*

3. Remove cap of cell and cut connecting metal tab with scissors, as shown in Figure 8.

Figure 8. *Cap is removed. Metal tab is cut to separate cap from case.*

4. Use pliers to pry back aluminum casing, starting at the top lip. Peel the material at a downward angle so that case can be removed in one continuous strip. A cell with the case partially peeled is shown in Figure 9.

Figure 9. *Aluminum case is removed by peeling it diagonally with pliers.*

5. Unroll electrodes and separate internal components of the cell, as shown in Figure 10.

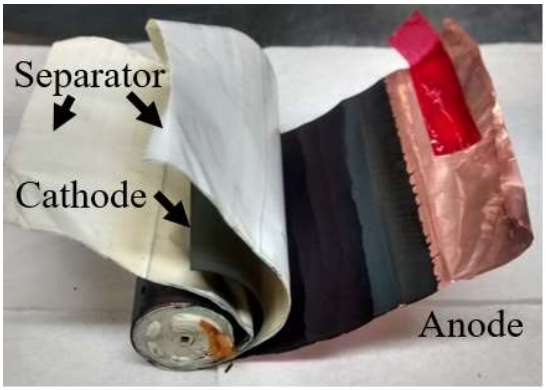

Figure 10. *Electrodes and separators are unrolled and pulled apart.*

6. Flatten electrodes and separators and examine for evidence of damage.

Scanning Electron Microscopy

Scanning electron microscopy (SEM) was used to examine the damage to externally shorted and overdischarged cell components. Images were also taken of the anode and cathode of a disassembled fresh cell to provide a baseline for comparison. Back-scattering electron (BSE) mode was used to verify that the material deposited on the cathode surface is copper, dissolved from the anodic current collector during the overdischarge process.

CHAPTER III

RESULTS

External Short Test

Voltage Response

Figure 11 shows the voltage response curves for external shorting using various resistors. For large resistors (1-100 Ω), shown in Figure 11a, the voltage decreases steadily throughout the discharge. As the size of the resistor increased, the current drawn from the battery decreased and the discharge phase took longer to complete. The shape of these voltage response curves matched the typical response of LIBs to constant resistance discharge.

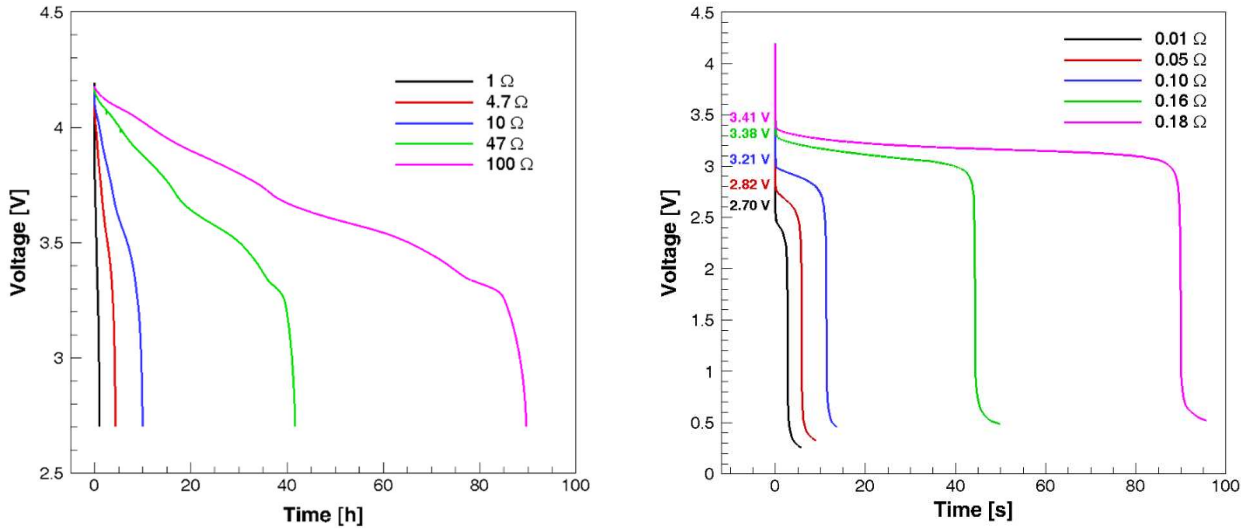

(a) (b)

Figure 11. *Voltage vs. Time curves during external short tests for (a) large resistors (1-100 Ω) and (b) small resistors (0.01-0.18 Ω)*

The shape of the curve changes for small resistors (0.01-0.18 Ω), shown in Figure 11b. The voltage drops instantaneously, remains at an intermediate level for a short time, then rapidly falls to almost 0 V. The initial voltage drop can be attributed to the Ohmic polarization associated with passing ionic current through a battery with an intrinsic internal resistance. When the cell was shorted by a small resistor, the high currents caused larger initial voltage drops. The second voltage drop can be attributed to a spike in concentration polarization after a short period of operation at high current. Concentration polarization is caused by the unavailability of the active species at the electrode/electrolyte interface. During normal operation, active particles diffuse to the electrode surface at a sufficient rate to supply the electrochemical reaction at the interface. When a cell is discharged too quickly, concentration gradients arise in the electrodes. A lack of active particles at the anode surface causes the anode voltage to rapidly rise, while a surplus of ions at the cathode surface causes the cathode voltage to fall. As a result, the full cell voltage decreases to nearly 0.0 V after only a few seconds of operation.

Current Response

The current response curves for external shorting using various resistors are shown in Figure 12. When constant resistance discharge is used, current decreases proportionally with voltage according to Ohm's law ($V=iR$). The result is that for large resistor trials, shown in Figure 12a, the current decreases steadily with voltage over time. For small resistor trials, shown in Figure 12b, the current spikes instantaneously at time of short, remains at an intermediate level for a short time, then falls close to zero for the remainder of the discharge.

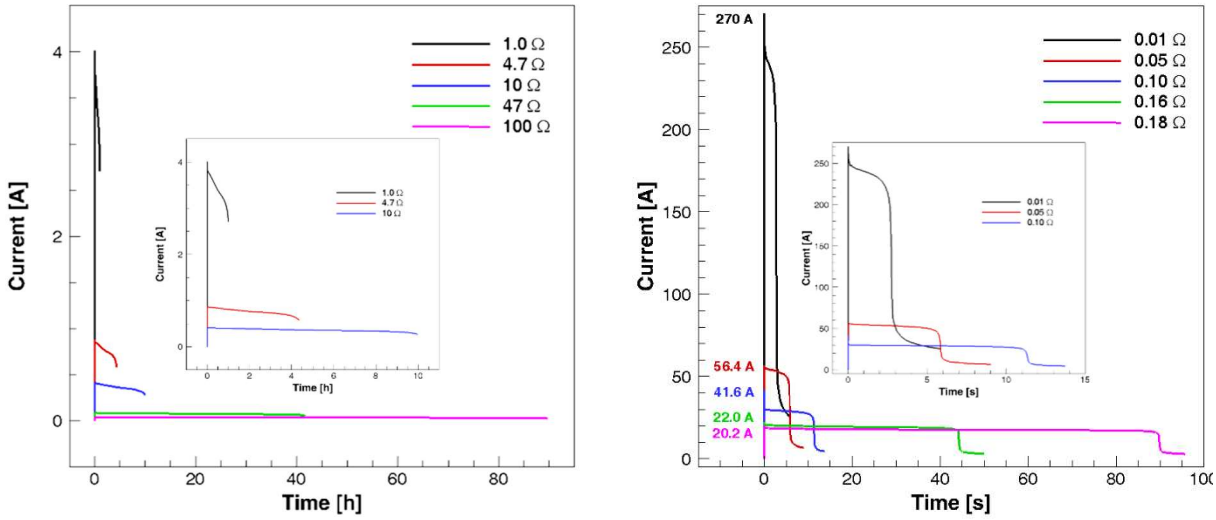

Figure 12. *Current vs. Time curves during external short tests for (a) large resistors (1-100* **Ω***) and (b) small resistors (0.01-0.18* **Ω**)

Temperature Response

The temperature response of the cell, measured by a K-type thermocouple attached to cell's exterior surface, is shown in Figure 13. Temperature is closely related to the internal heat generation rate, which can be estimated using the relation $P = i^2 R_{int}$, where P is power, i is current, and R_{int} is the internal resistance of the cell. Although a small increase in internal resistance is expected over many cycles, the main component influencing heat generation rate is the current.

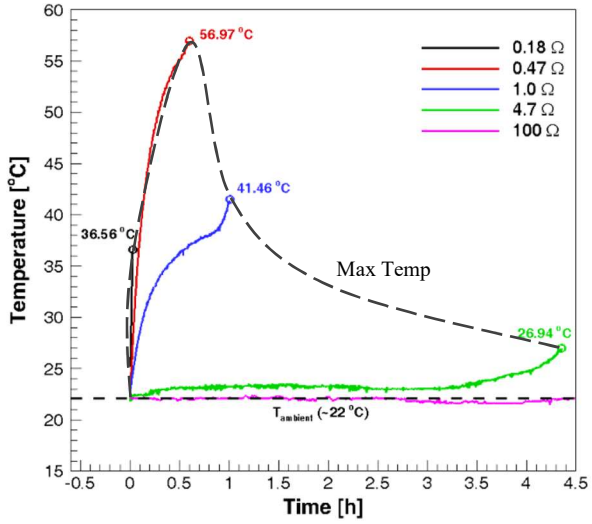

Figure 13. *Temperature vs. Time curves during external short for selected resistors.*

The highest temperature was achieved when an intermediate external resistance of 0.47 Ω was used. At resistances greater than 4.7 Ω, current is small, so the cell is able to dissipate heat to the environment nearly as fast as it is generated. Therefore, no substantial change in temperature was observed in the high-resistance trials. At resistances lower than 0.18 Ω, heat is generated at high rate during the initial current spike and the intermediate current plateau, but the heat generation rate quickly diminishes when concentration polarization causes the voltage to drop to nearly zero and the current to slow to a trickle. In this sense, the diffusion rate limitation of the electrochemical reaction serves as an in-built safety mechanism against thermal runaway during external shorting. For resistors between 0.18 Ω and 4.7 Ω, notable increases in temperature were observed on the cell surface, but no trials showed high enough temperatures to severely impact internal components.

Overdischarge and Copper Dissolution Test

The full voltage profile of the overdischarge test is shown in Figure 14. When the SOC is between 100% and 0%, the voltage resides in the normal voltage window specified by the manufacturer (2.5-4.2 V). Beyond 0% SOC lies the overdischarge region, where the cell voltage plummets to a minimum value of -1.3 V before rebounding asymptotically to 0 V. The rapid decline in cell voltage near 0% SOC can be attributed to the onset of concentration polarization, causing the anode voltage to rise and the cathode voltage to fall.

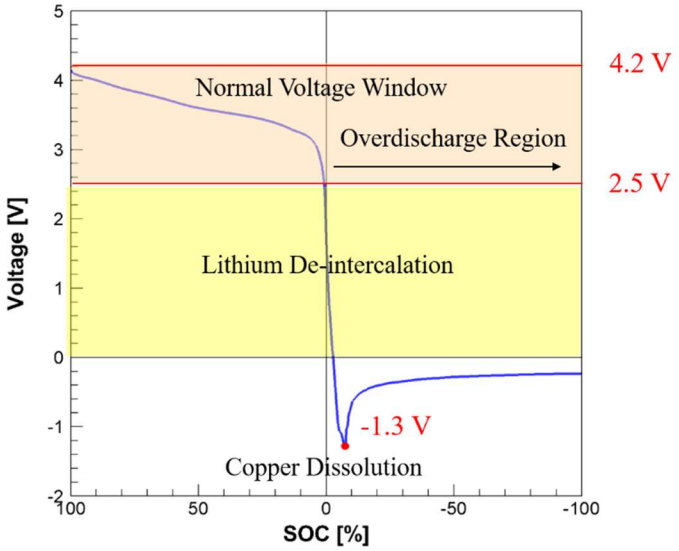

Figure 14. *Full voltage profile of overdischarge test, performed at 1C.*

The voltage profile for the overdischarge test can be roughly divided into four stages as drawn in Figure 15a. In Stage I, the voltage dropped rapidly to about -1 V, where it reached a distinct platform. In Stage II, the voltage continued to fall to its minimum value of -1.3 V. Stage III showed an increase in voltage with significant fluctuations, while in Stage IV, the voltage increased asymptotically to 0.0 V with very little fluctuation.

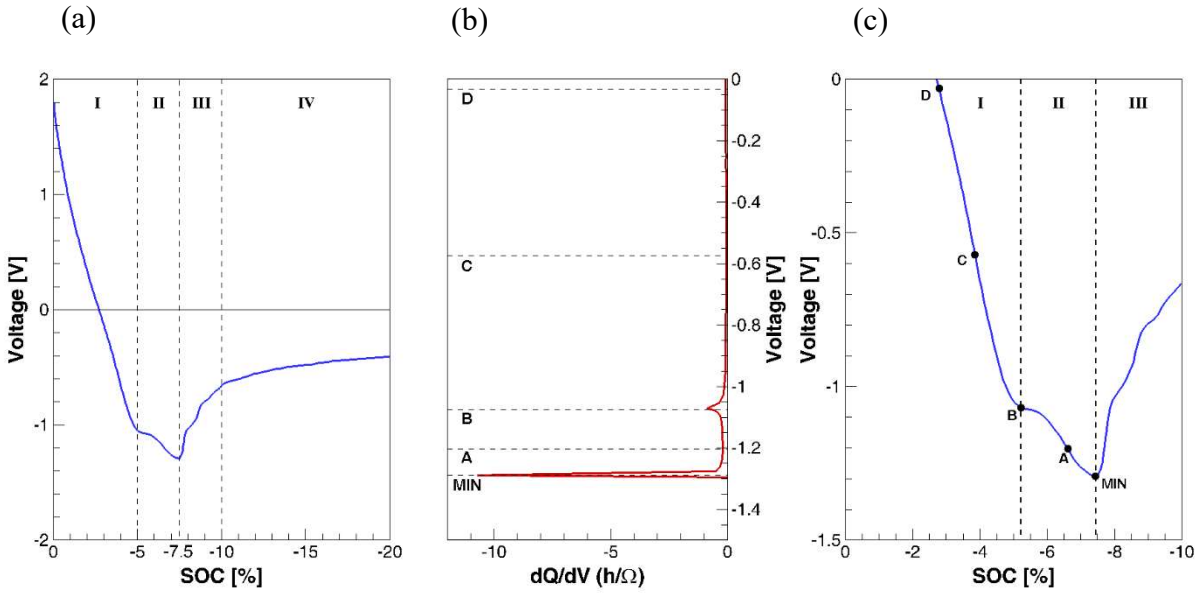

Figure 15. *Overdischarge voltage analysis. (a) Voltage profile during overdischarge, divided into four stages, (b) incremental capacity analysis of stages I and II with peaks and valleys marked, (c) close-up view of voltage profile with corresponding inflection points marked.*

The voltage decline in Stage I can be attributed to the increasing potential of the anode and the decreasing potential of the cathode as end-of-life concentration polarization takes effect. Throughout Stage I, the buildup of an ionic concentration gradient between the anode surface and the bulk material results in a rapid rise in anode voltage. Simultaneously, the lack of easily accessible interstitial sites in the cathode for new ions to reside causes the cathode voltage to fall. From the literature, it is known that copper dissolution and SEI breakdown begin when the anode voltage reaches around 3.5 V [10, 12]. This occurs at the start of Stage II, at approximately -5% SOC, where a significant peak in the incremental capacity analysis (shown in Figure 15b) signifies the occurrence of a phase change in the cell. The corresponding voltage plateau at -1.1 V, labeled point B in Figure 15c, can be accounted for by the overpotential for the initiation of copper

dissolution. Degradation of the copper current collector leads to an increase in charge transfer resistance in the anode, as the conductive pathway that transmits electrons to the external circuit grows thinner. The breakdown of the SEI throughout Stage II exposes the chemically reactive surface of graphite to the electrolyte. This reaction can also cause a large amount of heat generation and the release of gases within the cell, including carbon dioxide. Both copper dissolution and SEI breakdown further increase the anode voltage and decrease the voltage of the cell.

Upon reaching its minimum value of -1.3 V, the voltage begins to increase in Stage III with fluctuations. This corresponds to the depletion of lithium ions in the electrolyte. When the cathode voltage falls to around 3.5 V, Cu^{2+} ions in the electrolyte begin to deposit on the cathode surface, reducing the available reactive surface area on the electrode for reactive species. Stage III is characterized by the formation of copper crystals on the cathode surface. By the start of Stage IV, a uniform layer of copper begins to form and the cathode voltage stabilizes.

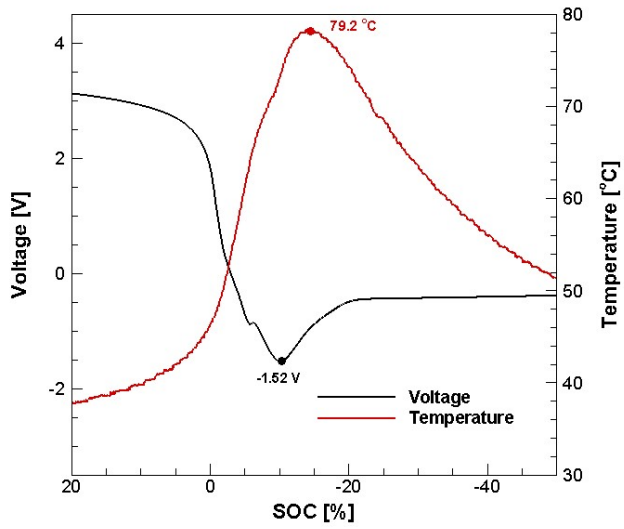

Figure 16. *Voltage and Temperature vs. SOC plot for overdischarge at 1C.*

The surface temperature of the cell is compared to the cell's voltage profile throughout the overdischarge test at 1C in Figure 16. Temperature begins to increase drastically around 0% SOC as concentration polarization sets in. The initiation of copper dissolution aligns with an inflection point in the temperature profile, showing that it further increased the heat generation rate. The temperature reached a maximum at 79.2ºC and declines as the voltage begins to approach 0 V. The cell that was overdischarged at C/10 experienced a temperature change of less than 20ºC, indicating that the temperatures achieved during overdischarge are rate-dependent. Although 79.2ºC is not a high enough temperature response to imply significant damage, a test performed at a higher discharge rate could result in higher temperatures as well.

Destructive Physical Analysis

Fresh Cell

In order to acquire a baseline for comparing results of the DPA, a fresh cell was opened. The unraveled cathode, anode, and separator surfaces of the fresh cell are shown in Figure 17. Both electrodes are smooth and black in the discharged state, although anode color varies with state of charge. The separator material is white on the anode-facing sides and tan on the cathode-facing sides due to the ceramic coating facing the cathode. This coating is intended to mitigate the consequences of lithium dendrite formation in the cell and prevent internal shorts from penetrating the separator.

(a) (b)

Figure 17. *Electrode and separator surfaces of (a) cathode and (b) anode of fresh 18650 cell after performing DPA.*

Externally Shorted Cell

The results of DPA on a cell that had been repeatedly externally shorted are shown in Figure 18. The bronze anode color seen in Figure 20b indicates that this cell was deconstructed in a partial state of charge. The main difference is the darkening of the separator material on both sides. This can possibly be attributed to the fracturing of electrode materials at the anode and cathode due to the high mechanical stresses induced during high-current operation. The loss of electrode material suggests that the external shorting caused a decrease in cell capacity. Nevertheless, it is important to note that this cell suffered repeated external shorting and could still be charged to full at 4.2 V.

(a) (b)

Figure 18. *Electrode and separator surfaces of (a) cathode and (b) anode of externally shorted 18650 cell after performing DPA.*

Overdischarge and Copper Dissolution Test

The DPA performed on the severely overdischarged cells showed much more obvious signs of damage than the externally shorted cell. Upon trying to unravel the electrode roll, the separator was unusually difficult to peel off of the cathode. When the layers were forced apart, parts of the ceramic coating on the separator adhered to the cathode surface instead, as shown in Figure 19. This adhesion is due to the deposition of copper particles on both surfaces, as the layers are pressed together tightly in the roll.

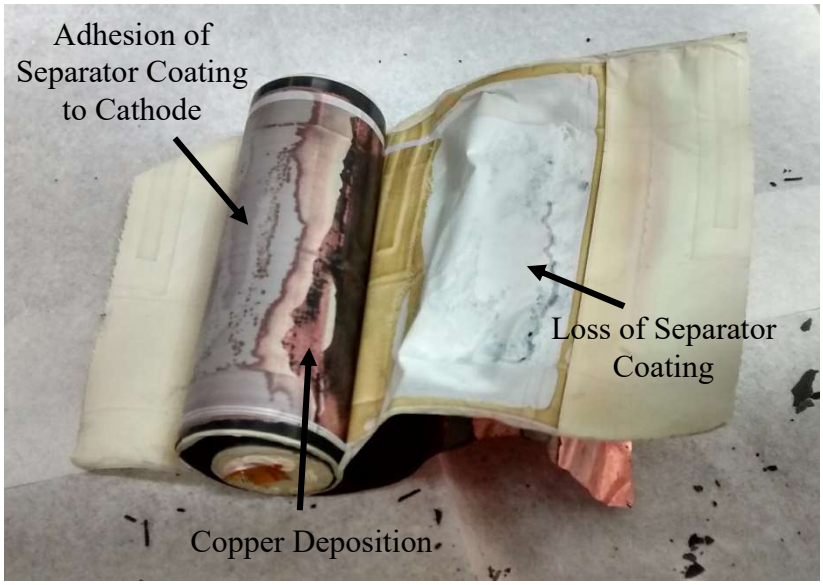

Figure 19. *Unraveling the electrode roll of an overdischarged cell.*

The center-facing side of the fully unraveled cathode roll and the corresponding separator are shown in Figures 20 and 21. The cathode can be divided into three zones, as labeled in Figure 21. In Zone A, the ceramic coating on the separator detached and stuck to the cathode. The coloring of Zone A suggests that a layer of copper below the ceramic is providing the adhesion. In Zone B, a layer of cathode material adhered to the separator, tearing away from the electrode. Zone C

represents a region where no material was ripped from either the electrode or separator surface, but a layer of copper deposition is visible. Samples from this region were taken for SEM post-mortem analysis to prove the presence of copper.

Figure 20. *Center-facing cathode surface and cathode-facing separators.*

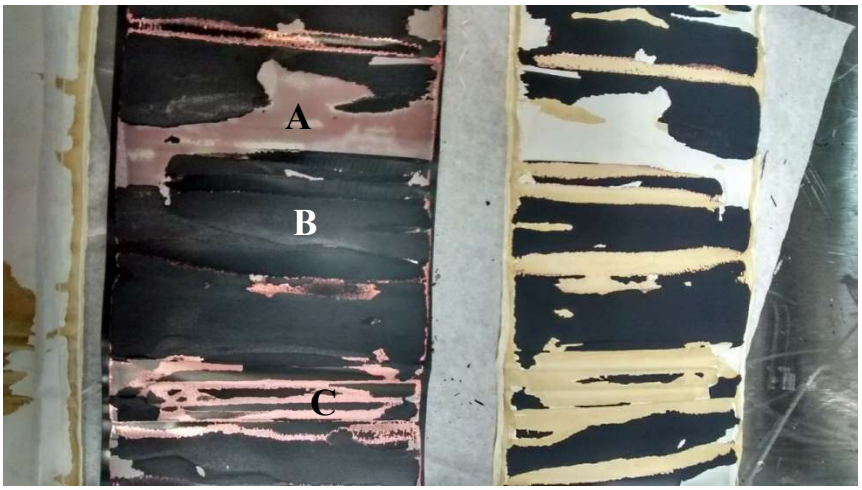

Figure 21. *Close-up center-facing cathode surface, aligned with the corresponding separator.*

In contrast to the center-facing cathode surface, the outward-facing surface, shown in Figure 22, was almost fully coated by the peeled separator coating. Beneath this layer, the reddish brown color indicates the deposition of a layer of copper. The copper on this face is more uniform

than on the center-facing surface and apparently thicker, as the detachment of the separator coating implies the deposition of copper on both the cathode and separator surfaces. The increased presence of copper on the outward-facing side of the cathode can be explained by the fact that the anode is the outermost layer of the electrode roll, which provides the source of copper.

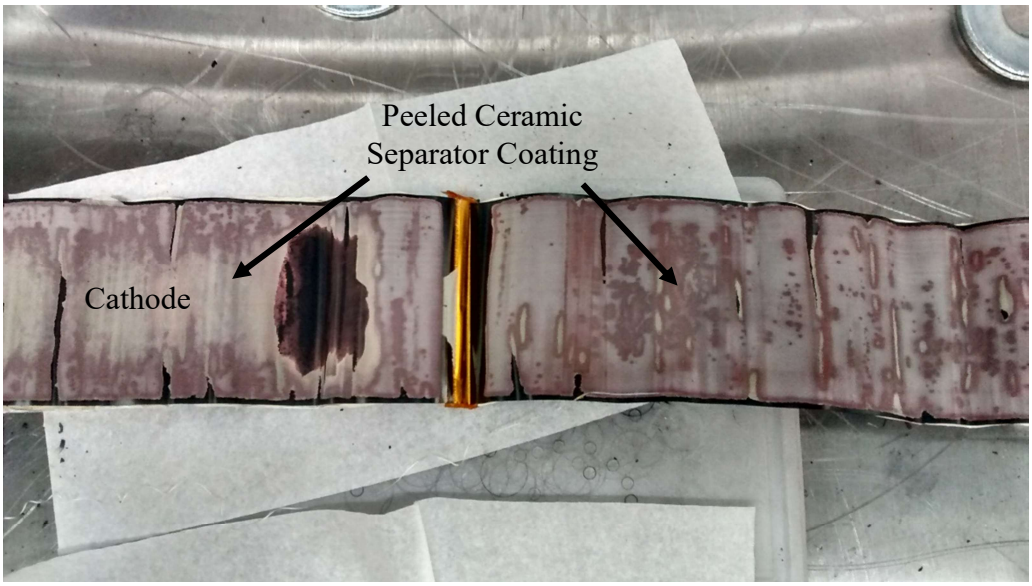

Figure 22. *Outward-facing cathode surface following extreme overdischarge.*

The anode of the overdischarged cell also suffered visible damage. Before it was unraveled, the graphite material surface appeared mostly undamaged, but several deep cracks were found in the roll, as shown in Figure 23. The dissolution of the copper current collector greatly reduces the mechanical stability of the anode while increasing the charge transfer resistance of the cell. Cracking also results in capacity loss and, in extreme cases, loss of electrical connection to the external circuit.

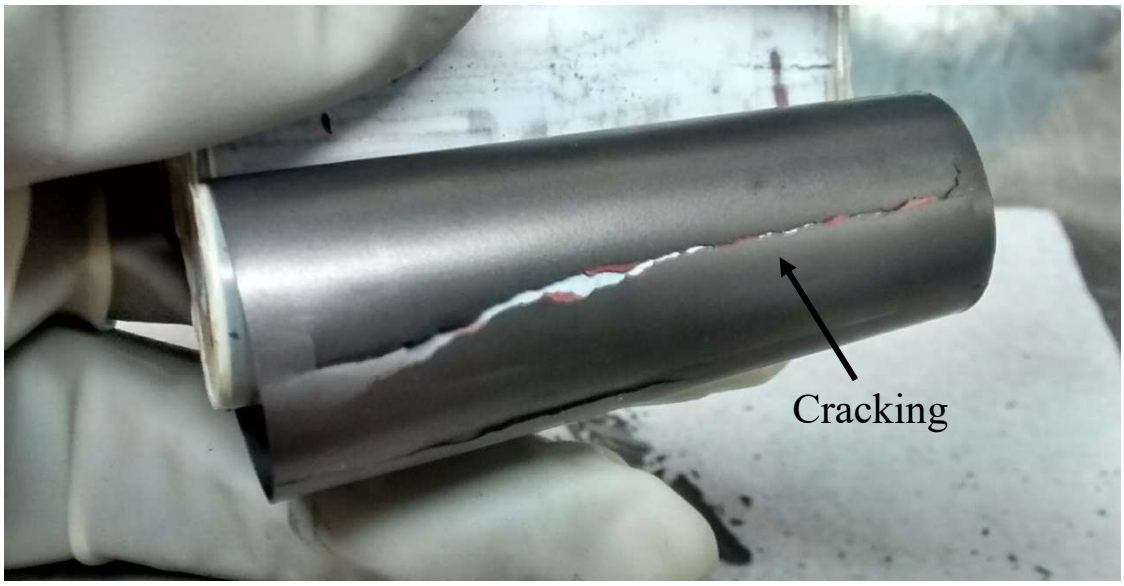

Figure 23. *Anode roll suffered from severe cracking before being unraveled.*

As the anode was unraveled, it was revealed that the remaining copper current collector was extremely thin and unstable. Much of the anode material crumbled under light stress as it was unraveled, leaving large gaps in the roll, as shown in Figure 24. Meanwhile, the anode-facing separator faces showed essentially no damage.

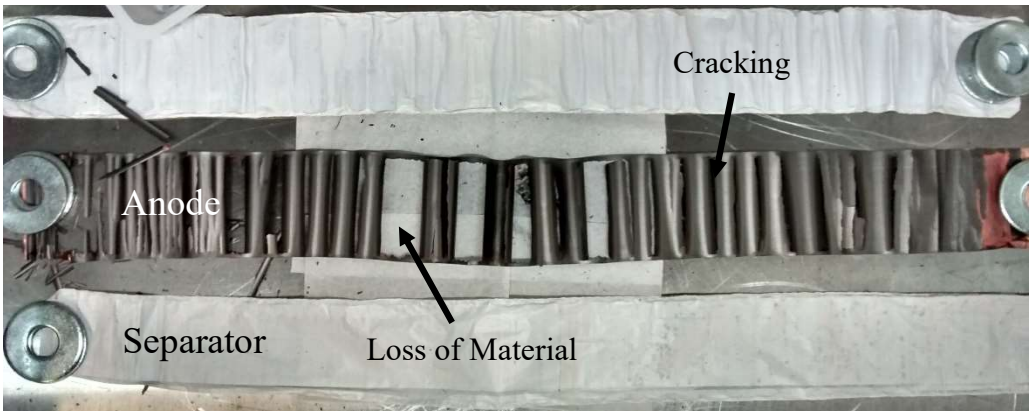

Figure 24. *Anode surface and anode-facing separator surfaces.*

Scanning Electron Microscopy

Fresh Cell

The damage caused to internal components during external shorting and overdischarge was examined post-mortem using scanning electron microscopy. To acquire a baseline for comparison of SEM results, images from a fresh cell's anode and cathode were acquired. The surface of a fresh cell anode at 1 kX zoom is shown in Figure 25.

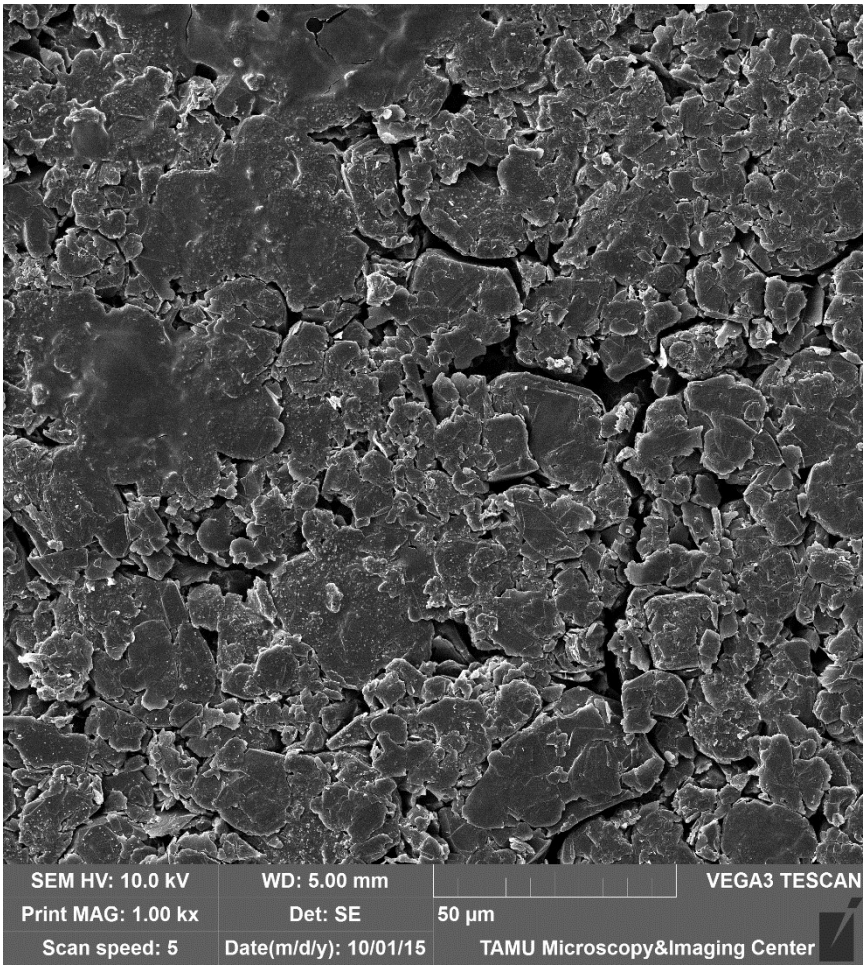

Figure 25. *SEM image of undamaged fresh cell anode material (graphite) at 1 kX.*

Externally Shorted Cell

An SEM image of the cathode surface of an externally shorted cell at 1 kX magnification is shown in Figure 26. The material surface is mainly intact, but shows the formation of some cracks due to the mechanical stresses of high-current operation and the rapid intercalation of ions into the material matrix. Cracking results in permanent reduction in cell capacity and a small increase in charge transfer resistance in the cathode.

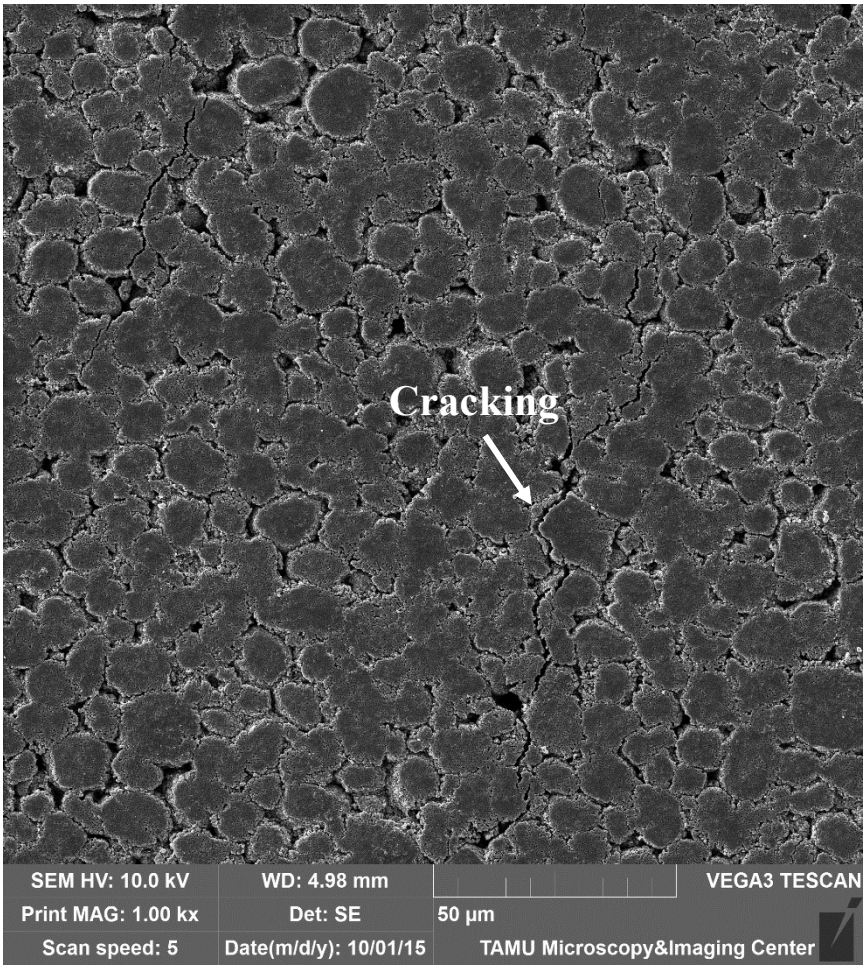

Figure 26. *SEM image of cathode surface of externally shorted cell at 1 kX.*

The anode surface of a cell that had suffered repeated external shorting was examined in Figure 27. The graphite shows sections with melted material, which is most likely the polymeric binder used to add stability to the anode slurry. The melting of this material can clog pores in the graphite where lithium ions could reside, thus reducing the capacity of the cell upon recharge. This also indicates that the cell was subjected to operation at high temperatures, which can lead to accelerated degradation.

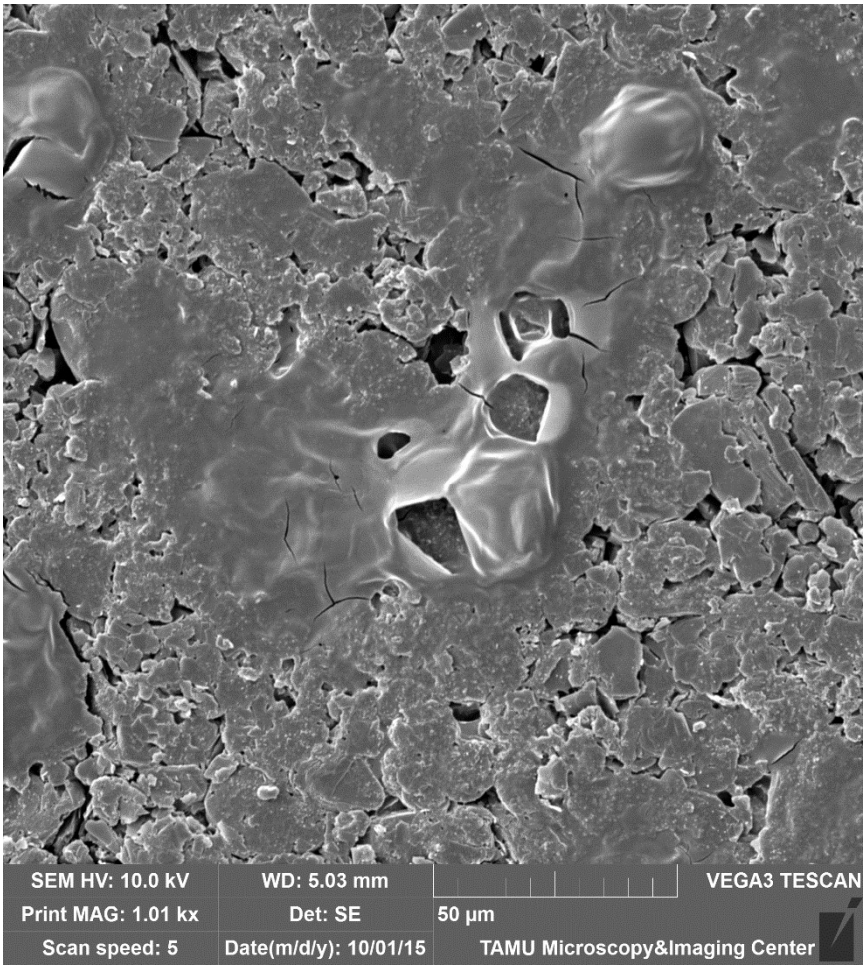

Figure 27. *SEM image of anode material of externally shorted cell at 1 kX, showing presence of melted binder material on surface.*

These tests confirm that although external shorting can cause some damage to cells, it is unlikely that a single incident of external shorting will cause a significant thermal threat to the cell or its surroundings. Shorting may cause some damage to cell components, which may result in capacity fade, but has not been shown to result in failure in any of our short duration tests.

Overdischarged Cell

The presence of copper on the cathode surface was confirmed by the SEM images shown in Figure 28. A back-scattered electron (BSE) detector was used to create these images, which produces images based on the number of electrons that collide with an atomic nucleus and are scattered back towards the detector. Since larger atoms have a higher probability of colliding with electrons, particles with greater atomic numbers appear brighter in the image. The copper crystals in Figure 28 are illuminated against the $LiNiCoAlO_2$ cathode surface, as the atomic number of copper exceeds any of the elements present in the cathode. The image also shows the presence of cracking in the cathode, most likely due to the stresses of forced intercalation of ions during overdischarge. Figure 28 is an image from the center-facing cathode surface, which was covered in copper more sparsely than the outward-facing surface.

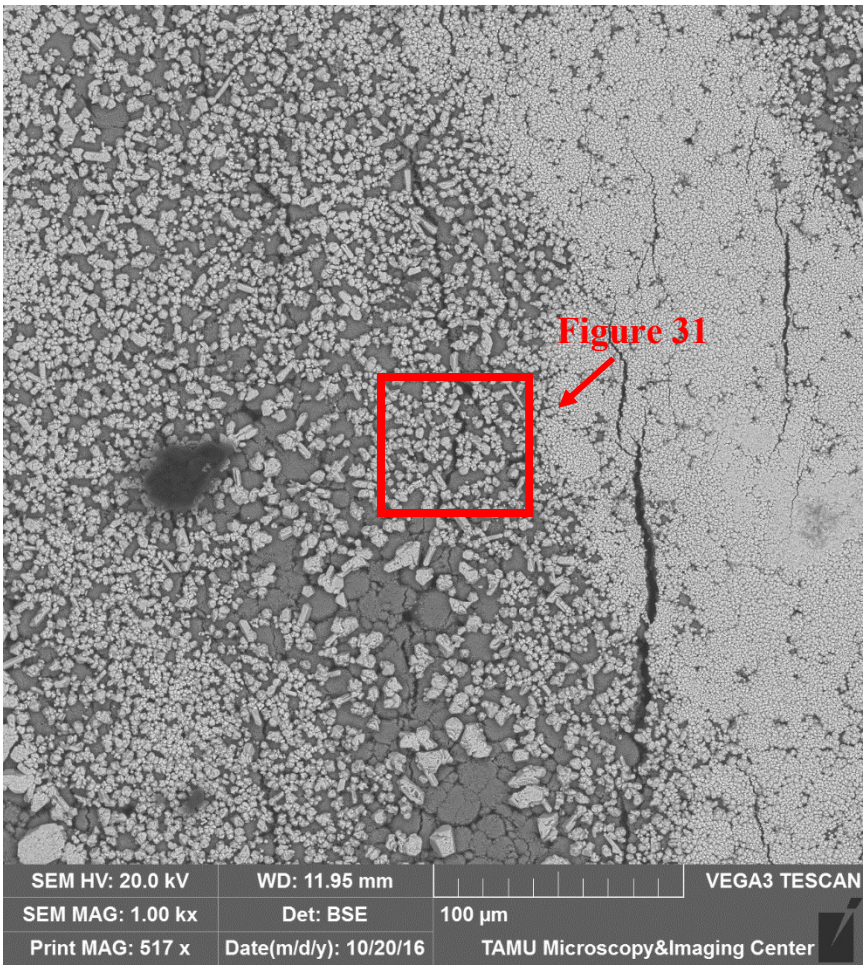

Figure 28. *SEM image of center-facing cathode surface using BSE at 1 kX.*

A section of the same cathode is examined at 5 kX magnification in Figure 29, which clearly highlights the formation of copper crystals on the cathode surface. In more densely coated areas of the cathode, the crystals merge to form a solid layer of copper that blocks the flow of lithium ion into or out of the electrode.

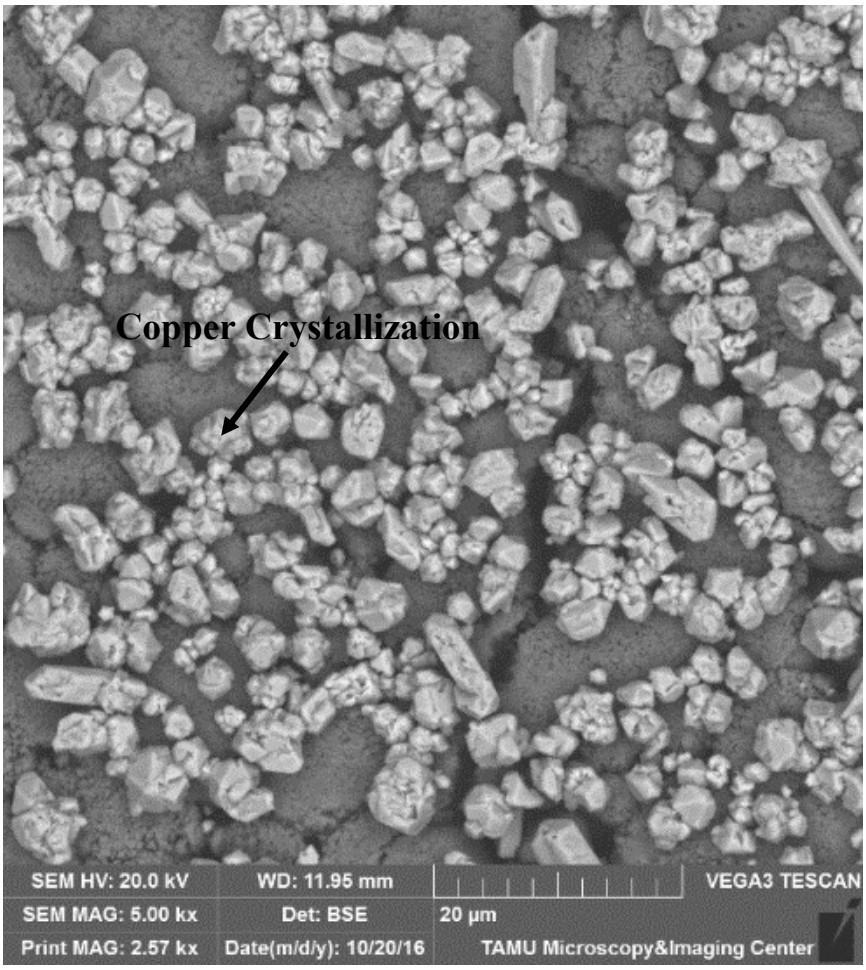

Figure 29. *SEM image at 5 kX of cathode of overdischarged cell with copper dissolution. BSE scan mode illuminates copper clusters.*

On the outward-facing cathode surface, most of the material was so densely coated in copper that it bonded the cathode to the ceramic coating of the separator. An image of the outward-facing cathode surface at 1 kX is shown in Figure 30. The left side of the image is a region coated in ceramic (SiO_2/Al_2O_3) with a thick layer of copper below it, while the right side is a region where a layer of cathode material was ripped off, exposing the bulk material. The region on the left shows how copper deposition can block access of ions to the electrolyte.

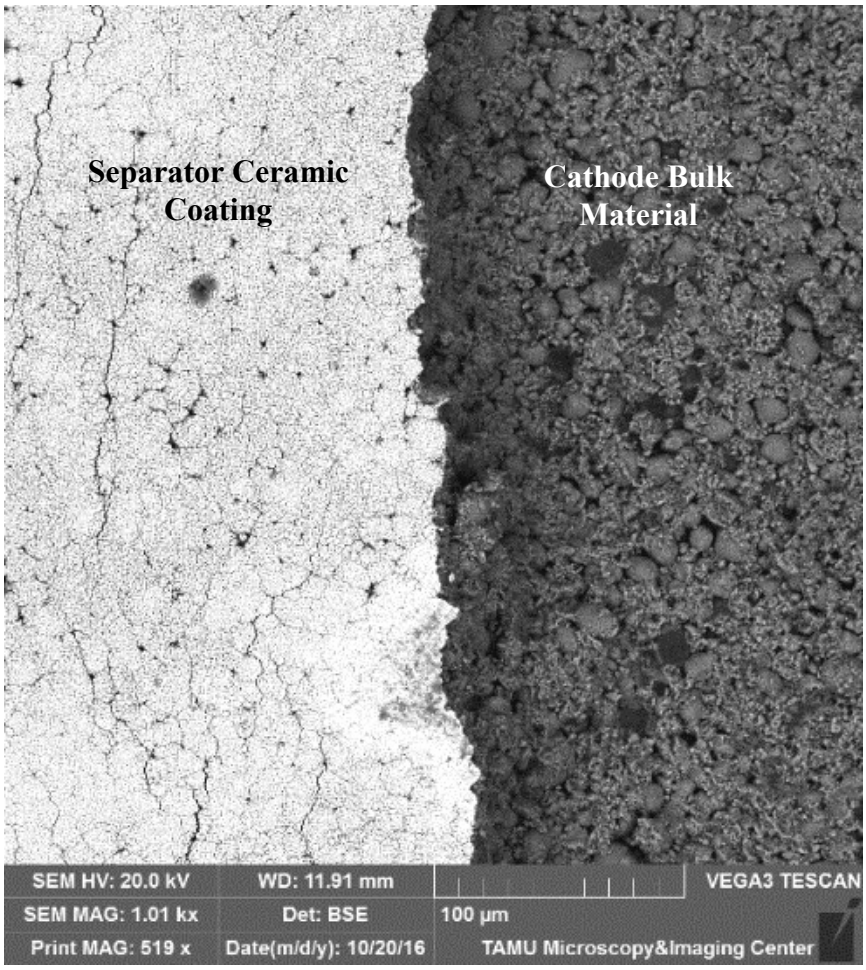

Figure 30. *SEM image of outward-facing cathode surface at 1 kX.*

Images of the anode of an overdischarged cell could not be acquired because efforts to prepare a sample caused a significant amount of damage due to the anode's poor mechanical stability. Therefore, an image could not be taken that accurately represented the state of the anode before it was unraveled.

CHAPTER IV

CONCLUSION

In this study, external shorting in commercial 18650 rechargeable lithium-ion cells was explored by studying constant resistance discharge behavior. Shorting the cell with very small resistance ($\leq$0.18 Ω) yields a response in which voltage and current fall to near-zero values after a short time due to the early onset of concentration polarization in the cell. It was found that shorting with resistances between 0.18 Ω and 4.7 Ω can cause significant increases in temperature because it allowed the cell to discharge with sustained high currents (20.2 A for 90 s at R=0.18 Ω). The greatest temperature rise occurred with the resistance of 0.47 Ω. The DPA of a cell that had been repeatedly short-circuited showed moderate damage to cell components. Separators appeared darker (destruction of the ceramic layer SiO_2/Al_2O_3) in the shorted cell, possibly due to fracturing of the cathode material during high-rate discharge. SEM images of the anode showed evidence of melting of the polymeric binder, while images of the cathode indicated the propagation of cracks on the surface. Fracturing, cracking, and melting of the binder all result in a permanent loss of capacity in the cell. Although anode voltage is known to rise during high-current operation, this study proves that copper dissolution cannot be induced via constant resistance discharge alone, regardless of the rate.

The results of the overdischarge test showed that extreme overdischarge conditions can lead to the dissolution of copper from the anodic current collector, which can lead to severe capacity loss and the deposition of metallic copper on the surface of the cathode and the cathode-facing separator faces. Copper dissolution has been shown to occur in commercial Panasonic NCR18650B cells at a voltage of -1.1 V. Guo *et al.* report that an internal short circuit begins to

form at this point, which allows the voltage to increase back to zero. This study differs from ours in that they attempted to recharge their cells at different SOC in order to determine where internal shorts begin to form. In the current study, recharge of cells was not attempted and no evidence of copper deposition was found on the anode or on the anode-facing side of the separators. This indicates that internal shorting due to the formation of copper dendrites in overdischarged cells is not a threat until recharge is attempted. When the electric field in the cell is reversed during charging, copper ions in the electrolyte that had not yet deposited on the cathode will instead deposit on the anode and could form conductive pathways.

Internally shorted cells in a large bank of cells can be dangerous because large amounts of heat are generated when recharge of a shorted cell is attempted. In severe cases, the high internal cell temperatures experienced during charging can lead to thermal runaway and can cause the cell to catch fire or explode. Therefore, cells that experience copper dissolution in modules should be immediately replaced upon detection. Without attempted recharge, cells were prone to failure due to blockage of the cathode's reactive surface by the deposited copper, as well as loss of electrical connection between the anode and external circuit due to cracking in the copper current collector. The cell that was overdischarged at a 1C rate experienced surface temperatures as high as 79.2ºC, indicating that temperatures at the center of the cell could be nearing the melting temperature of the separator (~130ºC for PE). If the separator were to melt, it would ideally flow into the pores of the electrodes and block current, but it also puts the cell at higher risk of internal shorting. Overdischarging at rates higher than 1C could therefore present a threat of achieving thermal runaway, although further testing would be required to determine this. This study demonstrates the need for balancing and monitoring systems in the design of large battery packs and modules, as one cell with an unbalanced voltage can lead to dangerous consequences for the whole system.

Future Work

In order to verify the electrochemical analysis of the overdischarge test, the test will be repeated in the future using a three-electrode 18650 cell. By measuring the anode and cathode voltages against a stable reference electrode, the relative contributions of each electrode can be examined throughout the overdischarge. The anode voltage profile will be of particular interest, as past studies have reported the onset of copper dissolution when the anode reaches ~3.5 V or above. A three-electrode test will also provide a more complete understanding of the battery behavior after the initiation of copper dissolution and the voltage profiles of the anode and cathode as the cell fails.

Although copper coloring was observed on the cathode surface during DPA and deposits of conductive material were observed via SEM, the presence of copper cannot be definitively determined by our present study. X-Ray Diffraction (XRD) will be performed on a sample of the cathode to prove that the material deposited on the cathode is, in fact, copper.

This study did not consider the effects of cell protections or cell geometry on overdischarge behavior. Removal of the positive temperature coefficient device (PTC) and current-interrupting device (CID) could affect cell behavior if either of these contributed to the cell failure. Future work may also consider using a pouch cell rather than a cylindrical cell to determine the influence of cell geometry on overdischarge response.

REFERENCES

[1] Huggins, R.A., *Advanced Batteries: Materials Science Aspects*, Springer Science + Business Media, LLC, (2009): 1-23.

[2] Huggins, R.A., *Energy Storage*, Springer Science + Business Media, LLC, (2010): 119-143.

[3] S. Tibken, R. Cheng, "Samsung answers burning Note 7 questions, vows better batteries," C*NET*, < www.cnet.com/news/samsung-answers-burning-note-7-questions-vows-betterbatteries>, (2017).

[4] Winter, Martin, and Ralph J. Brodd. "What are batteries, fuel cells, and supercapacitors?" *Chemical reviews* 104.10 (2004): 4245-4270.

[5] Linden, David. "Factors Affecting Battery Performance." *Handbook of Batteries* (2001): 3.1-3.24.

[6] Orendorff, Christopher J. "The role of separators in lithium-ion cell safety." *Electrochemical Society Interface* 21.2 (2012): 61-65.

[7] Aurbach, Doron, *et al*. "Design of electrolyte solutions for Li and Li-ion batteries: a review." *Electrochimica Acta* 50.2 (2004): 247-254.

[8] Lee, Hochun, *et al*. "Li2NiO2 as a novel cathode additive for overdischarge protection of Li-Ion batteries." *Chemistry of Materials* 20.1 (2007): 5-7.

[9] Guo, Rui, *et al*. "Mechanism of the entire overdischarge process and overdischarge-induced internal short circuit in lithium-ion batteries." *Scientific Reports* 6 (2016).

[10] Zhao, Mingchuan, *et al*. "Electrochemical Stability of Copper in Lithium-Ion Battery Electrolytes." *Journal of the Electrochemical Society* 147.8 (2000): 2874-2879.

[11] H. Maleki, J. Howard, "Effects of overdischarge on performance and thermal stability of a Li-ion cell." *Journal of Power Sources* 160 (2006): 1395-1402.

[12] C. Kishiyama, M. Nagata, T. Piao, J. Dodd, P.-N. Lam, H. Tsukamoto, Abs. 245, Proceedings of the 204th Electrochemistry Society Conference, Orlando FL, 2003.

[13] Z. Mao, Abs. 304, proceedings of the 206th Electrochemistry Society Conference, Honolulu, Hawaii 2006.

[14] Nitta, Naoki, *et al*. "Li-ion battery materials: present and future." *Materials Today* 18.5 (2015): 252-264.

[15] Tian, Huajun, *et al*. "High capacity group-IV elements (Si, Ge, Sn) based anodes for lithium-ion batteries." *Journal of Materiomics* 1.3 (2015): 153-169.

[16] Rahn, Christopher D., and Chao-Yang Wang. *Battery systems engineering*. John Wiley & Sons, (2013): 196-197.

[17] A. Bard, L. Faulkner, Electrochemical Methods – Fundamental and Applications, 2nd Edition, John Wiley and sons, (2000).

[18] F. La Mantia, *Characterization of Electrodes for Lithium-Ion Batteries through Electrochemical Impedance Spectroscopy and Mass Spectrometry*, Dissertation, ETH Zürich, (2008).

[19] Wu, Mao-Sung, *et al*. "Correlation between electrochemical characteristics and thermal stability of advanced lithium-ion batteries in abuse tests—short-circuit tests." *Electrochimica acta* 49.11 (2004): 1803-1812.

[20] Trevor V. Suslow, "Oxidation-Reduction Potential for Water Disinfection Monitoring, Control, and Documentation," University of California Davis, (2004).

[21] Leising, Randolph A., *et al*. "Abuse testing of lithium-ion batteries: Characterization of the overcharge reaction of LiCoO2/graphite cells." *Journal of The Electrochemical Society* 148.8 (2001): A838-A844.

[22] Venugopal, Ganesh. "Characterization of thermal cut-off mechanisms in prismatic lithium-ion batteries." *Journal of Power Sources* 101.2 (2001): 231-237.

[23] S. Erol, M. Orazem, R. Muller, “Influence of overcharge and over-discharge on the impedance response of $LiCoO_2$|C batteries.” *Journal of Power Sources* 270 (2014): 92-100.

[24] M. Zhao, “Electrochemical studies of lithium-ion battery anode materials in lithium-ion battery electrolytes.” Dissertation, Ohio University, 2001.

[25] D. Rahner, *J Power Sources*, 81, 358 (1999).

[26] N. N'dri, M. Megahed and S. D. Fabre, *Advanced Batteries, Accumulators and Fuel Cells (Abaf 12)*, 40, 205 (2012).